Supporting Information

Facile MOF Support Improvement in Synergy with Light Acceleration for Efficient Nanoalloy-Catalyzed H_2 Production from Formic Acid

Yue Liu,[a,b] Fangyu Fu,[c] Lionel Salmon,[d] Bruno Espuche,[e,f] Sergio Moya,[e] Murielle Berlande,[a] Jean-Luc Pozzo,[a] Jean-René Hamon,[b]* Didier Astruc[a]*

[a] Univ Bordeaux, ISM, UMR CNRS Nº 5255, 33405 Talence Cedex, France.
[b] Univ Rennes, CNRS, ISCR (Institut des Sciences Chimiques de Rennes) - UMR 6226, F-35000 Rennes, France.
[c] School of Chemistry and Chemical Engineering, Beijing Institute of Technology, Beijing, 102488, P. R. China.
[d] LCC, CNRS & University of Toulouse, 31077 Toulouse Cedex, France.
[e] Soft Matter Nanotechnology Lab, CIC biomaGUNE, Paseo Miramón 182. 20014. Donostia-San Sebastián, Gipuzkoa, Spain.
[f] POLYMAT, Applied Chemistry Department, Faculty of Chemistry, University of the Basque Country, UPV/EHU, Paseo Manuel de Lardizabal 3, Donostia-San Sebastián, 20018, Spain

Corresponding author E-mail : didier.astruc@u-bordeaux.fr

Table of Content

1. Materials and methods

- **Transmission Electron Microscopy (TEM)** and **high-resolution TEM (HRTEM)** were recorded using TEM JEOL JEM 1400 (120 kV)- 2100F.

- **Energy-dispersive X-ray Spectroscopy (EDS)** images were recorded using TEM-JEM-ARM200F Cold FEG equipped with an EDX spectrometer.

-**X-ray photoelectron spectra (XPS) System**: SPECS SAGE HR, X-Ray source: Mg Kα non-monochromatic, operated at 12.5 kV and 250 W. Take-off angle 90°, at ~10^{-8} Torr. Pass energy for survey spectra 30 eV, 15 eV for narrow scans. Analysis: spectra are calibrated to CC carbon 285 eV. Analysis consisted of Shirley background subtraction. Peaks are fitted with symmetrical Gaussian-Lorentzian (GL) line shapes. Samples were dispersed on a silica substrate, and its solvent was evaporated prior to measurement.

- **NMR spectra** were recorded at 25 °C with a Bruker AC 300, or 400 (300 or 400 MHz). All the chemical shifts are reported in parts per million (δ, ppm) with reference to Me_4Si for the 1H NMR spectra.

- **Inductively coupled plasma atomic emission spectroscopy (ICP-AES)**: Thermo Scientific iCAP 6300 DUO spectrometer with a 3-channel, 12-roller pump and a 27.12 MHz solid state RF plasma generator.

- **Brunauer-Emmet-Teller (BET)** areas were recorded with a 30% v/v N_2/He flow using pure N_2 (99.9%) as the internal standard. At least 2 cycles of N_2 adsorption-desorption in the flow mode were employed to determine total surface area using the standard single point method.

TOF determination:

TOF is defined as $TOF_{initial}$ calculated as follows:

$$\mathbf{TOF_{initial}} = \frac{P_{atm}V_{gas}/RT}{2n_{metal}t}$$

Where $TOF_{initial}$ is the initial turnover frequency when the conversion X_a reaches 20%, n_{metal} is the total molar number of metal in catalyst, and t is the reaction time when X_a reaches 20%.

2. Characterization and experimental data for the nanocatalysts

Table S1. Atomic ratios of ZIF-8@ Pd_2Ag_1@ZIF-67 measured by ICP-AES

Entry	Ag (ppm)	Pd (ppm)	Mass (mg)	Vol (ml)	Ag (wt%)	Pd (wt%)	Atomic ratios n_{Pd}: n_{Ag}
1	2.34	5.097	14.41	50	0.812	1.769	2.21: 1
2	2.916	4.846	13.35	50	1.092	1.815	1.7: 1

Table S2. Comparison of the TOF values with those of various nanocatalysts.

Nanocatalyst	T [K]	TOF [h^{-1}]	Reference
$Pd_1Ag_{1/2}$/NMP-450	303	332	[S1][1]
AgPd@Pd/TiO_2	300	201	[S2][2]
Ag@Pd	293	125	[S3][3]
Ag/Pd alloy	293	144	[S3][3]
Monodisperse $Ag_{42}Pd_{58}$/C	323	382	[S4][4]
Monodisperse $Au_{41}Pd_{59}$/C	323	230	[S5][5]
Pd_5Ag_5 NWs@g-C_3N_4 (with light)	298	420	[S6][6]
PdAu/rGO	353	129.6	[S7][7]
ZIF-8@Pd_2Ag_1@ZIF-67 (in dark)	353	245	This work
ZIF-8@Pd_2Ag_1@ZIF-67 (with light)	353	430	This work

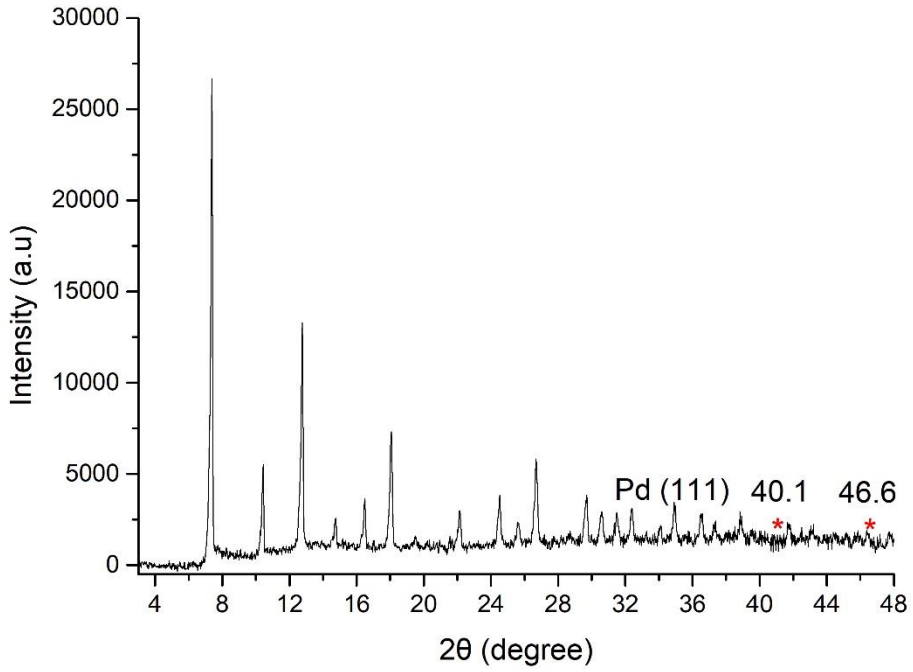

Figure S1. X-ray diffraction patterns of ZIF-8@Pd_2Ag_1@ZIF-67.

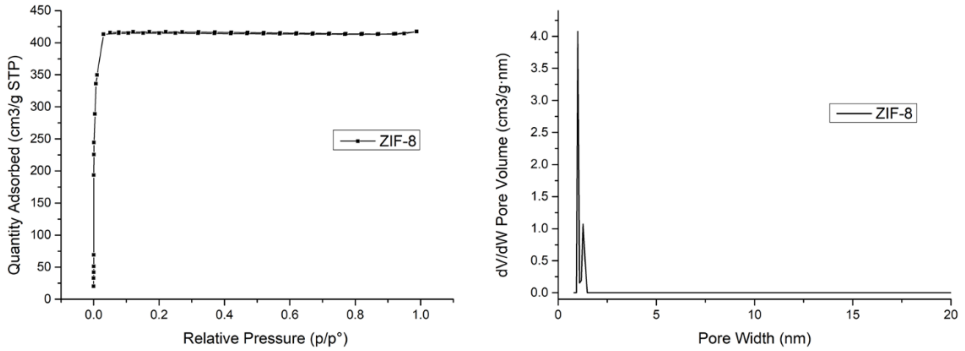

Figure S2. N_2 adsorption-desorption isotherms and DFT pore distribution of ZIF-8.

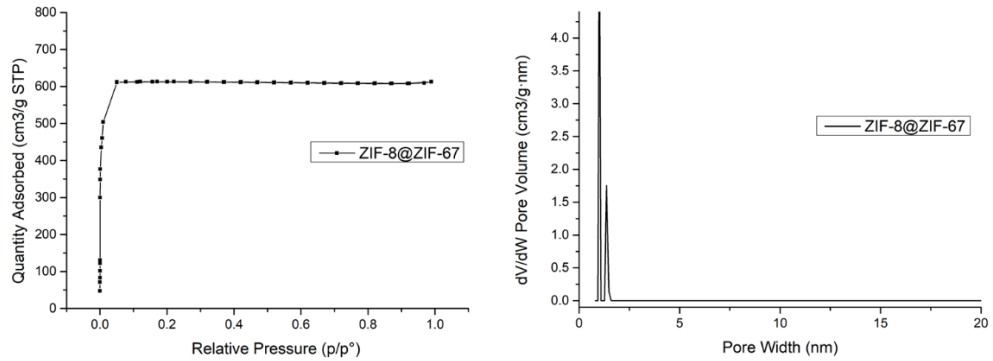

Figure S3. N_2 adsorption-desorption isotherms and DFT pore distribution of ZIF-8@ZIF-67.

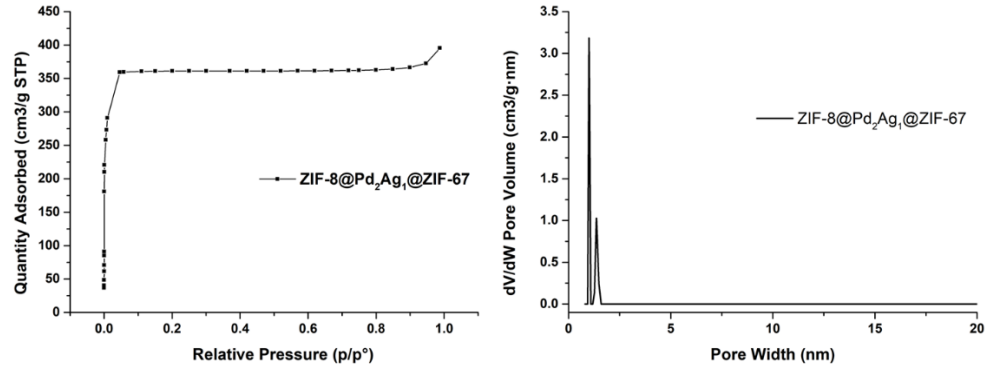

Figure S4. N_2 adsorption-desorption isotherms and pore distribution of ZIF-8@Pd_2Ag_1@ZIF-67 determined by DFT.

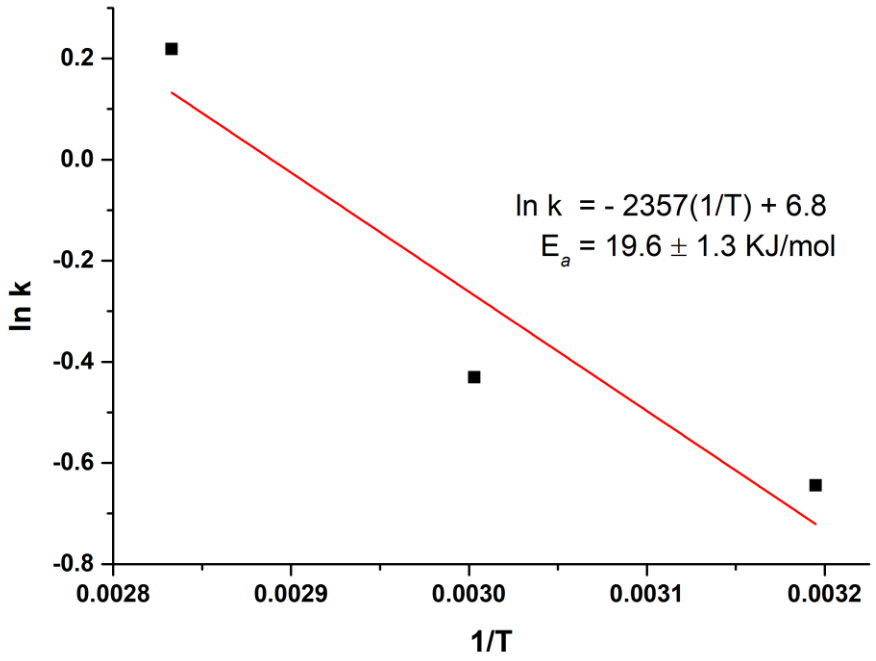

Figure S5. Arrhenius plots in FA dehydrogenation catalyzed by ZIF-8@Pd_2Ag_1@ZIF-67 at different temperatures.

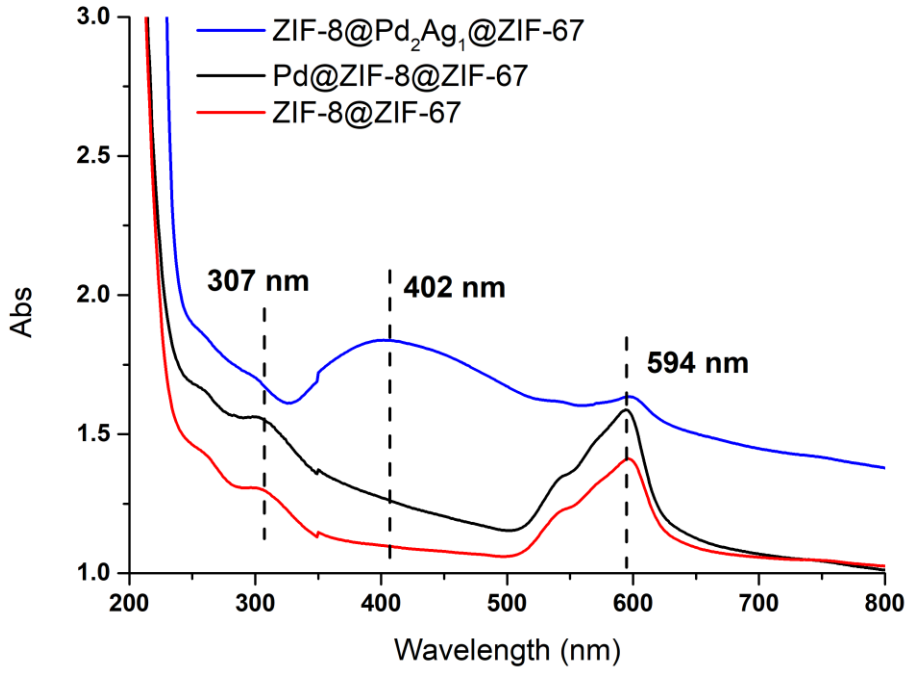

Figure S6. UV-vis. spectra of ZIF-8@ZIF-67, Pd@ZIF-8@ZIF-67, and ZIF-8@Pd_2Ag_1@ZIF-67.

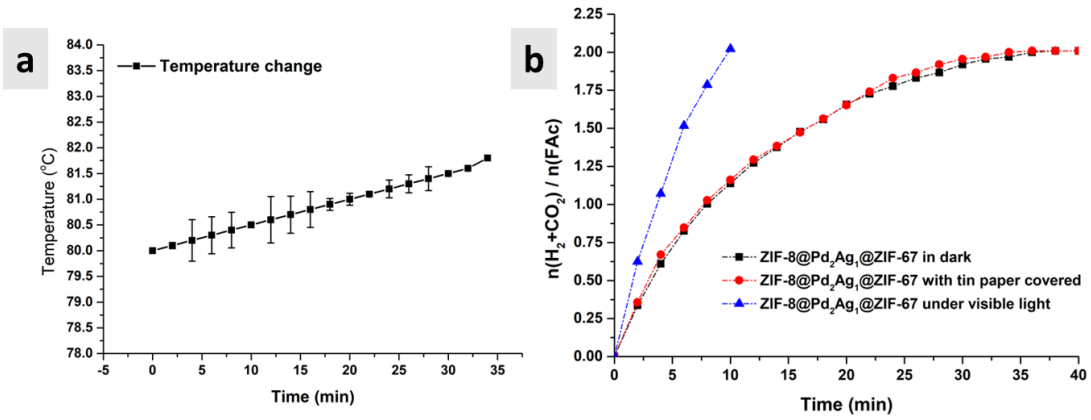

Figure S7. (a) temperature change under visible light irradiation and (b) catalytic efficiency under different conditions

References

(S1)Tian, Z.; Dong, C.; Li, D.; Wang, G.-H. Palladium-Based Bimetallic Catalysts for Highly Selective Semihydrogenation of Alkynes Using Ex Situ Generated Hydrogen. *Mater. Today Chem.* **2021**, *20*, 100467. DOI: 10.1016/j.mtchem.2021.100467.

(S2) Hattori, M.; Shimamoto, D.; Ago, H.; Tsuji, M. AgPd@Pd/TiO_2 Nanocatalyst Synthesis by Microwave Heating in Aqueous Solution for Efficient Hydrogen Production from Formic Acid. *J. Mater. Chem. A.* **2015**, *3* (20), 10666–10670. DOI: 10.1039/C5TA01434D.

(S3) Tedsree, K.; Li, T.; Jones, S.; Chan, C. W. A.; Yu, K. M. K.; Bagot, P. A. J.; Marquis, E. A.; Smith, G. D. W.; Tsang, S. C. E. Hydrogen Production from Formic Acid Decomposition at Room Temperature Using a Ag–Pd Core–Shell Nanocatalyst. *Nat. Nanotechnol.* **2011**, *6* (5), 302–307. DOI: 10.1038/nnano.2011.42.

(S4) Zhang, S.; Metin, Ö.; Su, D.; Sun, S. Monodisperse AgPd Alloy Nanoparticles and Their Superior Catalysis for the Dehydrogenation of Formic Acid. *Angew. Chem. Int. Ed.* **2013**, *52* (13), 3681–3684. DOI: 10.1002/anie.201300276.

(S5) Metin, Ö.; Sun, X.; Sun, S. Monodisperse Gold–Palladium Alloy Nanoparticles and Their Composition-Controlled Catalysis in Formic Acid Dehydrogenation under Mild Conditions. *Nanoscale* **2013**, *5* (3), 910–912. DOI: 10.1039/C2NR33637E.

(S6) Liu, H.; Liu, X.; Yang, W.; Shen, M.; Geng, S.; Yu, C.; Shen, B.; Yu, Y. Photocatalytic Dehydrogenation of Formic Acid Promoted by a Superior PdAg@g-C_3N_4 Mott–Schottky Heterojunction. *J. Mater. Chem. A.* **2019**, *7* (5), 2022–2026. DOI: 10.1039/C8TA11172C.

(S7) Grad, O.; Mihet, M.; Coros, M.; Dan, M.; Lazar, M. D.; Blanita, G. Reduced Graphene Oxide Modified with Noble Metal Nanoparticles for Formic Acid Dehydrogenation. *Catal. Today* **2021**, *366*, 41–47. DOI: 10.1016/j.cattod.2020.08.009.